PAPER

Neuromorphic CMOS Circuits Implementing a Novel Neural Segmentation Model Based on Symmetric STDP Learning

Eric Shun Fukuda[1], Gessyca Maria Tovar[2], Tetsuya Asai[2], Tetsuya Hirose[2] and Yoshihito Amemiya[2]

[1]Graduate School of Frontier Sciences, The University of Tokyo
Kashiwanoha 5-1-5, Kashiwa-shi, Chiba 277-8561, Japan
Phone:+81-4-7136-3873, Fax: +81-4-7136-3873 E-mail: fukuda@iba.k.u-tokyo.ac.jp

[2]Graduate School of Information Science and Technology, Hokkaido University
Kita 14, Nishi 9, Kita-ku, Sapporo 060-0814, Japan
Phone:+81-11-706-7147, Fax:+81-11-706-7890

Abstract **We designed a simple neural segmentation model that is suitable for analog circuit implementation. The model consists of excitable neural oscillators and adaptive synapses, where learning is governed by a symmetric spike-timing dependent plasticity (STDP). We numerically demonstrated basic operations of the proposed model as well as fundamental circuit operations using a simulation program with integrated circuit emphasis (SPICE).**

Keywords: Neuromophic VLSI, spiking neurons, spike-timing dependent plasticity

1. Introduction

Humans can distinguish multiple sensory sources that coincide. Recent discoveries of synchronous oscillations in the visual and auditory cortex have triggered much interest in exploring oscillatory correlation in order to solve neural segmentation problems. Many neural models that perform segmentation have been proposed, [1–3], but they are often difficult to implement on practical integrated circuits. Recently, a neural segmentation model called LEGION (Locally Excitatory Globally Inhibitory Oscillator Networks) [4] has been attracting attention because it can be easily implemented on circuits [5]. However, not including learning of neurons, under certain conditions the LEGION model does not work. For example, if one object is in the presence of noise or shadow, even if neurons are stimulated at the same time, segmentation occurs, resulting in many different fragments. In other words, the LEGION model fails to work in the presence of noise, This problem is solved in our network by including learning as well as all-to-all connections of neurons.

We have developed a simple neural segmentation model for analog complementary metal-oxide-semiconductor (CMOS) circuits. It includes learning and is suitable for applications such as figure-ground segmentation and the cocktail-party effect, among others. The model consists of mutually coupled neural oscillators exhibiting synchronous (or asynchronous) oscillations. All the neurons are coupled with each other through positive or negative synaptic connections. Each neuron accepts external inputs such as sound inputs in the frequency domain, and oscillates (or does not oscillate) when the input amplitude is higher (or lower) than a given threshold value. Our basic idea is to strengthen (or weaken) the synaptic weights between synchronous (or asynchronous) neurons, which may result in phase-domain segmentation. The synaptic weights are updated on the basis of symmetric spike-timing dependent plasticity (STDP) using Reichardt's correlation neural network [6], which is suitable for analog CMOS implementation.

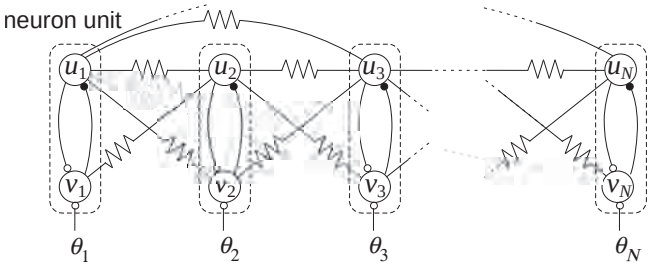

Fig. 1 Network construction of segmentation model

In the following sections, we introduce our segmentation model and demonstrate the operations through numerical simulations. Then we present unit CMOS circuits for our model and demonstrate the operations using a simulation program with integrated circuit emphasis (SPICE).

2. Model and Basic Operations

Our segmentation model is illustrated in Fig. 1. The network has N neural oscillators consisting of the Wilson-Cowan type activator and inhibitor pairs (u_i and v_i) [7]. All the oscillators are coupled with each other through resistive synaptic connections, as illustrated in the figure. The dynamics are defined by

$$\tau \frac{du_i}{dt} = -u_i + f_{\beta_1}(u_i - v_i) + \sum_{j \neq i}^{N} W_{ij}^{\mathrm{uu}} u_j \quad (1)$$

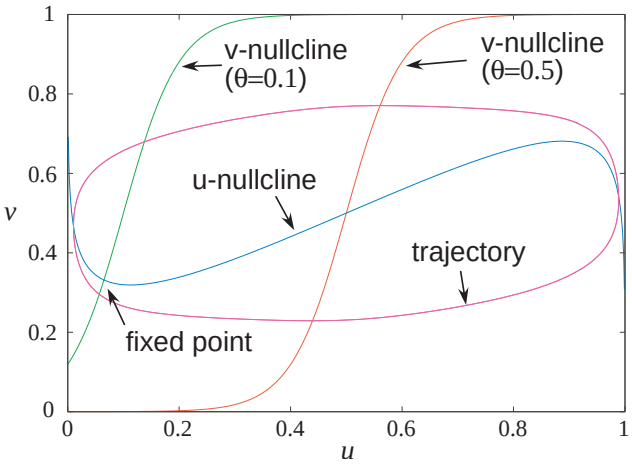

Fig. 2 Nullclines and trajectories of single neural oscillator

$$\frac{dv_i}{dt} = -v_i + f_{\beta_2}(u_i - \theta_i) + \sum_{j \neq i}^{N} W_{ij}^{\mathrm{uv}} u_j \quad (2)$$

where τ represents the time constant, N is the number of oscillators, and θ_i the external input to the i-th oscillator. Furthermore, $f_{\beta_i}(x)$ represents the sigmoid function defined by $f_{\beta_i}(x) = [1 + \tanh(\beta_i x)]/2$, W_{ij}^{uu} is the connection strength between the i-th and j-th activators and W_{ij}^{uv} is the strength between the i-th activator, and the j-th inhibitor. The nullclines of a single oscillator ($W_{ij}^{\mathrm{uu}} = W_{ij}^{\mathrm{uv}} = 0$) for different θ's (0.1 and 0.5) and trajectories for $\theta = 0.5$ are shown in Fig. 2. The remaining parameters were set at $\tau = 0.1$, $\beta_1 = 5$ and $\beta_2 = 10$. Models in which the dynamics are described by Eqs. (1) and (2), are suitable for implementation in analog very large scale integrations (VLSIs) because the sigmoid function can be implemented in such VLSIs by using differential-pair circuits.

According to the stability analysis in [7], the i-th oscillator exhibits excitable behaviors when $\theta_i < \Theta$ where $\tau \ll 1$ and $\beta_1 = \beta_2$ ($\equiv \beta$), and where Θ is given by

$$\begin{aligned} \Theta &= u_0 - \frac{2}{\beta}\tanh^{-1}(2v_0 - 1) \quad (3) \\ u_0 &\equiv \frac{1 - \sqrt{1 - 4/\beta}}{2} \\ v_0 &\equiv u_0 - \frac{2}{\beta}\tanh^{-1}(2u_0 - 1) \end{aligned}$$

and the oscillator exhibits oscillatory behaviors when $\theta_i \geq \Theta$, if W_{ij}^{uu} and W_{ij}^{uv} for all i and j are zero.

Suppose that neurons are oscillating ($\theta_i \geq \Theta$ for all i) with different initial phases. The easiest way to segment these neurons is to connect the activators belonging to the same (or different) group with positive (or negative) synaptic weights. In practical hardware; however, corresponding neuron devices have to be connected by special devices with both positive and negative resistive properties,

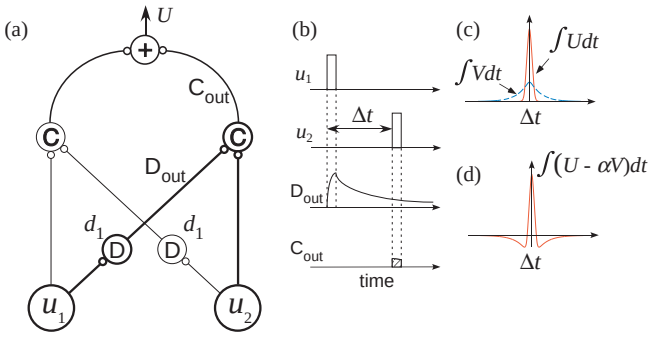

Fig. 3 Reichardt's correlation neural network

which prevent us from designing practical analog circuits. Therefore, we used positive synaptic weights between activators and inhibitors and not negative weights. When the weight between the i-th and j-th activators (W_{ij}^{uu}) is positive and W_{ij}^{uv} is zero, the i-th and j-th activators are synchronized. Contrarily, when the weight between the i-th activator and the j-th inhibitor (W_{ij}^{uv}) is positive and W_{ij}^{uu} is zero, the i-th and j-th activators exhibit asynchronous oscillation because the j-th inhibitor (synchronous to the i-th activator) inhibits the j-th activator.

The synaptic weights (W_{ij}^{uu} and W_{ij}^{uv}) are updated on the basis of our assumption that one neural segment is represented by synchronous neurons and is asynchronous with respect to neurons in the other segment. In other words, neurons should be correlated (or anti-correlated) if they receive synchronous (or asynchronous) inputs. These correlation values can easily be calculated by using Reichardt's correlation neural network [6], which is suitable for analog circuit implementation [8]. The basic unit is illustrated by thick lines and circles in Fig. 3(a). The unit consists of a delay neuron (D) and a correlator (C). A delay neuron produces blurred (delayed) output D_{out} from spikes produced by activator u_1. The dynamics are given by

$$d_1 \frac{dD_{\mathrm{out}}}{dt} = -D_{\mathrm{out}} + u_1 \quad (4)$$

where d_1 represents the time constant. The correlator accepts D_{out} and spikes produced by activator u_2 and outputs $C_{\mathrm{out}} = D_{\mathrm{out}} \times u_2$. The conceptual operation is illustrated in Fig. 3(b). Note that C_{out} qualitatively represents correlation values between activators u_1 and u_2 because C_{out} is decreased (or increased) when Δt (inter-spike intervals of the activators) is increased (or decreased). Since this basic unit can be used to calculate correlation values only for positive Δt, we used two basic units, which we call a unit pair, as shown in Fig. 3(a). The output (U) is thus obtained for both positive and negative Δt by summing the two C_{out}s. Through temporal integration of U, we obtained impulse responses of this unit pair. The sharpness is increased as $d_1 \to 0$. Two impulse responses for small and large d_1 (red and blue curves) are plotted in Fig. 3(c). Introducing two unit pairs with different time constants,

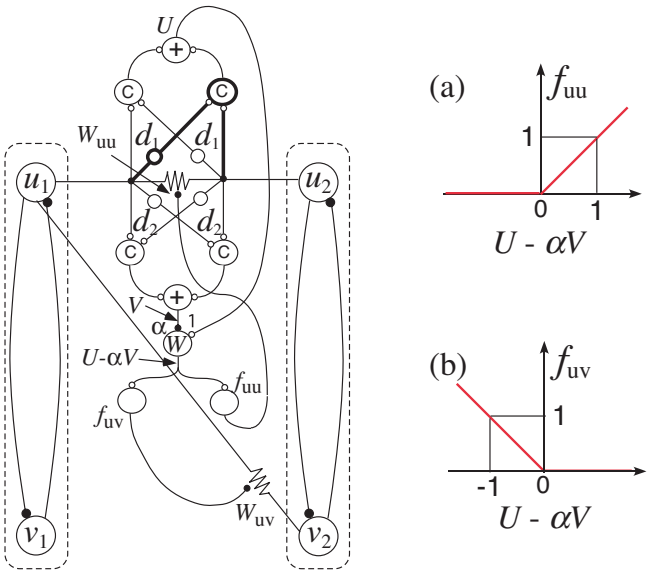

Fig. 4 STDP learning circuitry

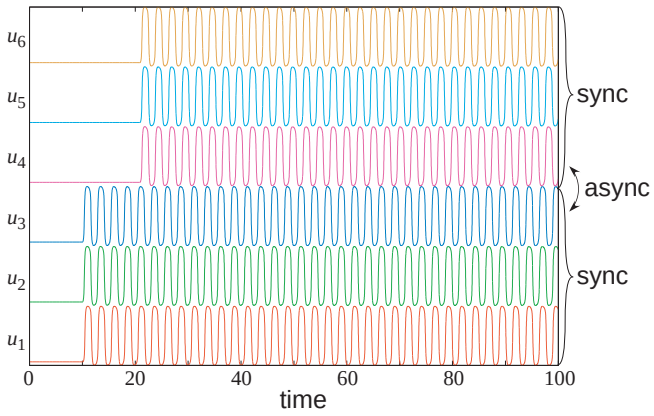

Fig. 5 Numerical simulation results

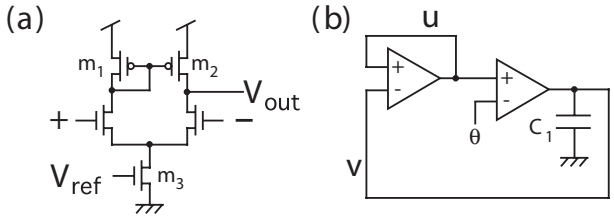

Fig. 6 Unit circuits for neural segmentation: (a) differential amplifiers and (b) neural oscillator

i.e., d_1 and d_2 ($\gg d_1$), one can obtain the two impulse responses (U and V) simultaneously. The weighted subtraction ($U - \alpha V$) produces well-known Mexican hat characteristics, as shown in Fig. 3(d). We used this symmetric characteristic for the weight updating as spike-timing dependent plasticity (STDP) in the oscillator network.

A schematic of our learning circuitry is shown in Fig. 4. The two unit pairs are located between activators u_1 and u_2. The weighted subtraction ($U - \alpha V$) is performed by interneuron W. According to our above assumptions for neural segmentation, when $U - \alpha V$ is positive, the weight between activators u_1 and u_2 (illustrated by a horizontal resistor symbol in Fig. 4) is increased because the activators should be correlated. On the other hand, when $U - \alpha V$ is negative, the weight between activator u_1 and inhibitor v_2 (illustrated by a slant resistor symbol in Fig. 4) is increased because activators u_1 and u_2 should be anti-correlated. To this end, the output of interneuron W is given to two additional interneurons ($f_{\rm uu}$ and $f_{\rm uv}$). The input-output characteristics of these interneurons are shown in Figs. 4(a) and (b). Namely, $f_{\rm uu}$ (or $f_{\rm uv}$) increases linearly when positive (or negative) $U - \alpha V$ increases but is zero when $U - \alpha V$ is negative (or positive). Those positive outputs ($f_{\rm uu}$ and $f_{\rm uv}$) are given to the weight circuit in order to modify the positive resistances. The dynamics of the "positive" weight between activators u_i and u_j is given by

$$\frac{dW_{ij}^{\rm uu}}{dt} = -W_{ij}^{\rm uu} + f_{\rm uu} \qquad (5)$$

and the "positive" weight between activator u_i and inhibitor v_j is given by

$$\frac{dW_{ij}^{\rm uv}}{dt} = -W_{ij}^{\rm uv} + f_{\rm uv} \qquad (6)$$

We performed numerical simulations with $N = 6$, $\tau = 0.1$, $\beta_1 = 5$, $\beta_2 = 10$, $d_1 = 2$, $d_2 = 0.1$ and $\alpha = 1.2$. Time courses of activators u_i ($i = 1 \sim 6$) are shown in Fig. 5. Initially, the external inputs θ_i ($i = 1 \sim 6$) were zero ($< \Theta$), but θ_i for $i = 1 \sim 3$ and $i = 4 \sim 6$ were increased to 0.5 ($> \Theta$) at $t = 10$ s and 20.9 s, respectively. We observed that $u_{1\sim3}$ and $u_{4\sim6}$ were gradually desynchronized without breaking synchronization among neurons in the same group, which indicates that segmentation of neurons on the basis of the input timing was successfully achieved.

3. CMOS Unit Circuits and Operations

Our Wilson-Cowan based neural oscillators have been implemented in [7]. The oscillator uses standard differential amplifiers shown in Fig. 6(a) which consists of a differential pair (+ and -), a current mirror (m_1 and m_2), and a bias transistor (m_3). The construction of an entire neural oscillator including additional capacitor C_1 is illustrated in Fig. 6(b). The simulated nullclines of a single neuron circuit for different θs (0.5 V and 2.5 V) and trajectories for $\theta = 2.5$ V with $C_1 = 10$ pF and $V_{\rm ref} = 2$ V are shown in Fig. 7. Transient simulation results of the neuron circuit are shown in Fig. 8. Time courses of the activator (u) and inhibitor (v) units are shown in (a) and (b), respectively. In (a), θ was initially set at 0.5 V (in a relaxing state), and u did not oscillate. Then θ was increased to 2.5 V at t = 0.1

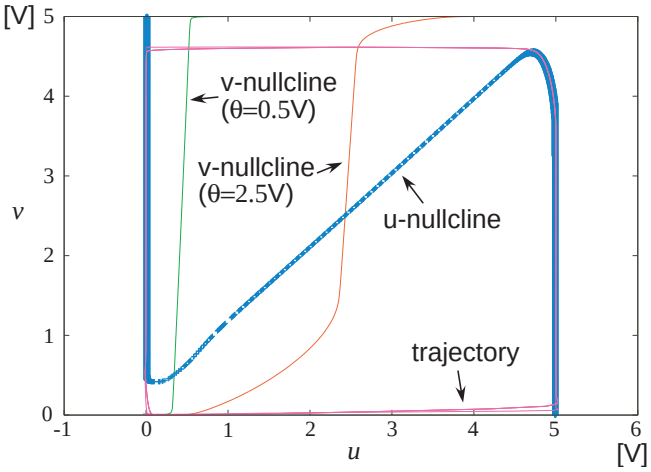

Fig. 7 Nullclines and trajectory for $\theta = 2.5$ V obtained from circuit simulations

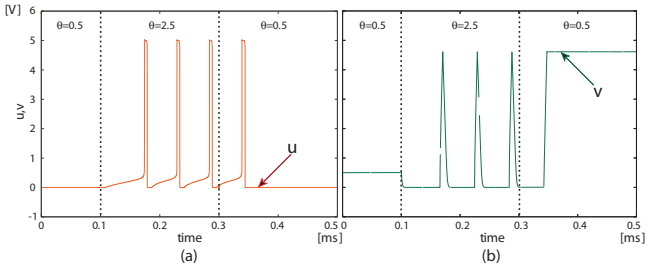

Fig. 8 Simulation results of neural oscillator

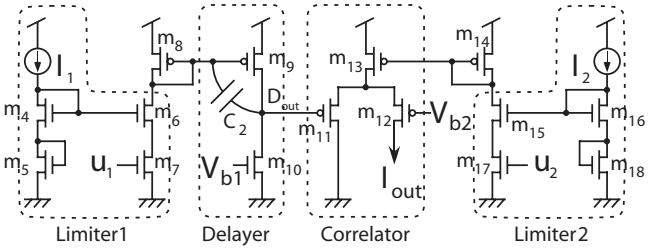

Fig. 9 STDP circuit

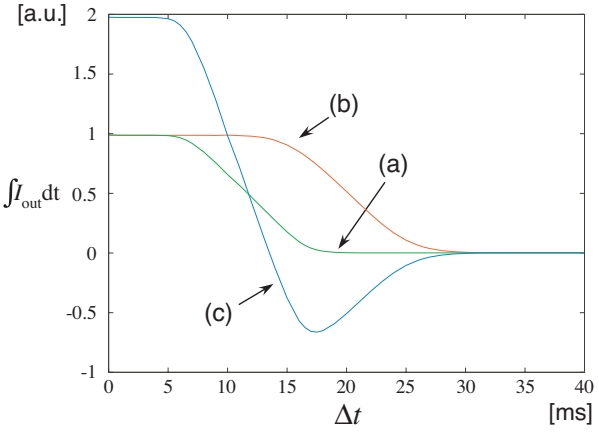

Fig. 10 Ideal STDP characteristics without limiters

ms, and u exhibited stiff oscillations. Again, θ was set at 0.5 V at t = 0.3 ms. Since u had been excited before this time, the neuron emitted one spike and then relaxed, as expected. In (b), with θ first set at 0.5 V v did not oscillate. Then θ was increased to 2.5 V at t = 0.1 ms, and v started to oscillate. Again, θ was set at 0.5 V at t = 0.3 ms. Since v had been already excited the neuron emitted one spike, but unless unit u the inhibitor unit v stayed at high level.

A circuit implementing Reichardt's basic unit, which is shown in Fig. 3(a), is shown in Fig. 9. For practical purposes, we added two limiters that convert voltage pulses of u_1 and u_2, which vary from 0 to $V_{\rm dd}$, into subthreshold current pulses. The bias current I_1 drives m_4 and m_5. Transistor m_6 is thus biased to generate I_1 because m_4 and m_6 share the gates. When m_7 is turned on (or off) by applying $V_{\rm dd}$ (or 0) to u_1, I_1 is (or is not) copied to m_8. Transistors m_8 and m_9 form a current mirror, whereas m_9 and m_{10} form a pMOS source-common (inverting) amplifier in which the gain is increased as $V_{\rm b1} \to 0$. Since parasitic capacitance C_2 is significantly amplified by this amplifier, temporal changes of u_1 are blurred on the amplifier's output ($D_{\rm out}$). Therefore, this "delayer" acts as a delay neuron, as shown in Fig. 3(a). A correlator circuit consists of a pMOS differential pair (m_{11} and m_{12}) and a bias transistor (m_{13}). When $u_2 = V_{\rm dd}$ (or zero), I_2 is (or is not) copied to m_{13} through m_{15} to m_{18}, as explained above. Therefore, output current $I_{\rm out}$ is obtained only when $u_2 = V_{\rm dd}$. Under this condition, $I_{\rm out}$ is proportional to $D_{\rm out} - V_{\rm b2}$ for small $|D_{\rm out} - V_{\rm b2}|$. This operation corresponds to that of a correlator in Fig. 3(a).

We carried out circuit simulations of the above circuits. The parameter sets we used for the transistors were obtained from MOSIS AMIS 1.5-μm CMOS process. Transistor sizes of m_1, m_2, m_3, m_{13} and m_{14} were fixed at $L = 16$ μm and $W = 4$ μm to construct accurate current mirrors. The length and width of the resting transistors were set at 1.6 μm and 4 μm, respectively. The supply voltage was set at 5 V.

Simulation results of our STDP circuits are shown in Figs. 10 and 11. In Fig. 10, ideal current pulses (amplitude: 100 nA, pulse width: 10 ms) were used instead of limiters as shown in Fig. 9. Parameters C_2, V_{b1}, and V_{b2} were set at 100 fF, -0.2 V, and 3.7 V, respectively. The value of V_{b2} was set at the intermediate value between m_{11}'s maximum and minimum gate voltage, and this causes the differential pair's output to vary the most. The value of V_{b1} was chosen so that the delayer makes a reasonable delay. Horizontal axes (Δt) in Figs. 10 and 11 represent time intervals of input current pulses (spikes). We integrated $I_{\rm out}$ during the simulation and plotted normalized values [(a) in Fig. 10]. Then we changed the value of V_{b_1} to -2 V. The lowered V_{b1} reduced the drain current

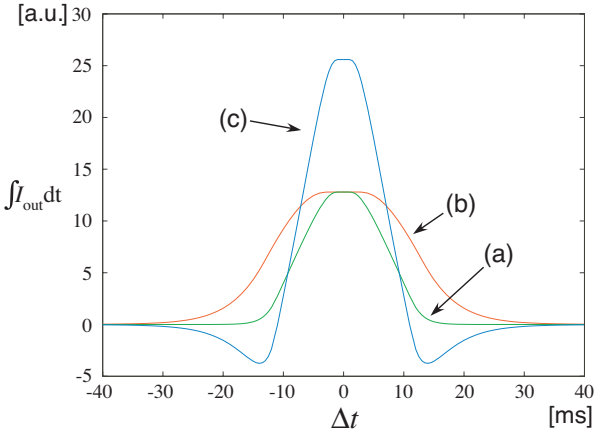

Fig. 11 Symmetric STDP characteristics with limiters

of m_{10} and increased the delay. Again, $I_{\rm out}$ was integrated and normalized. The result is plotted [(b) in Fig. 10]. The larger delay made the integrated $I_{\rm out}$ converge to zero at a larger Δt. By subtracting (b) from tripled (a), we obtained half characteristics of STDP learning [(c) in Fig. 10]. In Fig. 11, voltage pulses (amplitude: 5 V, pulse width: 10 ms) were applied to u_1 and u_2 in Fig. 9. Parameters C_2 and V_{b2} were set at 5 pF and 3.7 V, respectively. The integrated $I_{\rm out}$s are plotted in Fig. 11(a) for $V_{b1} = 0$ and Fig. 11(b) for $V_{b1} = -0.04$ V. The result was qualitatively equivalent to the STDP characteristics shown in Fig. 3(d).

4. Conclusion

We developed a simple neural segmentation model that is suitable for analog CMOS implementation. First, instead of using negative weights required for anti-correlated oscillation among different segments, we introduced positive connections between activators and inhibitors among different neuron units. Second, we proposed a novel segmentation method based on symmetric spike-timing dependent plasticity (STDP). The STDP characteristics were produced by combining Reichard's correlation neural networks, which are suitable for analog CMOS implementation. Our proposed segmentation network was demonstrated through numerical simulations. Basic circuits for constructing segmentation hardware were developed and evaluated. We showed that our circuit could produce symmetric STDP characteristics. A disadvantage of the model is that neurons are all-to-all connected. The high number of connections makes implementing the model on circuits difficult. Hence, our next target includes reducing the number of connections, designing the complete segmentation model, and implementing the network on CMOS VLSIs.

Acknowledgments

This study was partly supported by the Industrial Technology Research Grant Program in '04 from New Energy and Industrial Technology Development Organization (NEDO) of Japan, and a Grant-in-Aid for Young Scientists [(B)17760269] from the Ministry of Education, Culture Sports, Science and Technology (MEXT) of Japan.

References

[1] Ch. von der Malsburg and W. Schneider: A neural cocktail-party processor, Biological Cybernetics, Vol. 54, pp. 29-40, 1986.

[2] Ch. von der Malsburg and J. Buhmann: Sensory segmentation with coupled neural oscillators, Biological Cybernetics, Vol. 67, pp. 233-242, 1992.

[3] S. K. Han, W. S. Kim and H. Kook: Temporal segmentation of the stochastic oscillator neural network, Physical Review, E, Vol. 58, pp. 2325-2334, 1998.

[4] D.L. Wang and D. Terman: Locally excitatory globally inhibitory oscilator networks, IEEE Trans. on Neural Networks, Vol. 6 No. 1, pp, 283-286, 1995.

[5] H. Ando, T. Morie, M. Nagata and A. Iwata: A Nonlinear Oscillator Network for Gray-Level Image Segmentation and PWM/PPM Circuits for Its VLSI Implementation, IEICE Trans. Fund. Electron. Comm. Comp. Sci., Vol. E83-A, No. 2, pp. 329-336, 2000.

[6] W. Reichardt: Principles of Sensory Communication (Wiley, New York, 1961) p. 303.

[7] T. Asai, Y. Kanazawa, T. Hirose and Y. Amemiya: Analog reaction-diffusion chip imitating the Belousov-Zhabotinsky reaction with Hardware Oregonator Model, International Journal of Unconventional Computing, Vol. 1, No. 2, pp. 123-147, 2005.

[8] T. Asai, M. Ohtani and H. Yonezu: Analog MOS circuits for motion detection based on correlation neural networks, Japanese Journal of Applied Physics, Vol. 38, No. 4B, pp. 2256-2261, 1999.

Eric Shun Fukuda received the B.S. degree from Hokkaido University, Hokkaido, Japan, in 2006. Currently he is master student in the Department of Frontier Informatics at the University of Tokyo. His research interests include studies in the field of Artificial Life.

Gessyca Tovar was born in Venezuela in 1981. She received the B.S. degree in Electronic Engineering from Jose Antonio Paez University, Venezuela, in 2004. Currently she is working towards her Master degree in the Department of Electrical Engineering at Hokkaido University, Japan. Her research interests include neuromorphic computation and

hardware implementation.

Testuya Hirose received the B.S., M.S. and Ph.D. degrees from Osaka University, Osaka, Japan, in 2000, 2002, and 2005, respectively. Currently, he is a Research Associate in the Department of Electrical Engineering, Hokkaido University, Sapporo, Japan. His current research interests are in low-power analog/digital CMOS circuits and subthreshold MOSFET functional circuits for intelligent sensors. Dr. Hirose is a member of the Institute of Electronics, Information and Communication Engineers of Japan, and the IEEE.

Tetsuya Asai is an Associate Professor in the Graduate School of Information Science and Technology, Hokkaido University, Sapporo, Japan. His research interests concentrate around developing nature-inspired integrated circuits and their computational applications. Current topics that he is involved with include; intelligent image sensors that incorporate biological visual systems or cellular automata in the chip, neuro chips that implement neural elements (neurons, synapses, etc.) and neuromorphic networks, and reaction-diffusion chips that imitate vital chemical systems.

Yoshihito Amemiya received the B.E., M.E., and Ph.D. degrees from the Tokyo Institute of Technology, Tokyo, Japan, in 1970, 1972, and 1975. He joined NTT Musashino Laboratories in 1975, where he worked on the development of silicon process technologies for high-speed logic LSIs. From 1983 to 1993, he was with NTT Atsugi Laboratories and developed bipolar and CMOS circuits for Boolean logic LSIs, neural network LSIs, and cellular automaton LSIs. Since 1993, he has been a Professor with the Department of Electrical Engineering, Hokkaido University, Sapporo. His research interests are in the fields of silicon LSI circuits, signal processing devices based on nonlinear analog computation, logic systems consisting of single-electron circuits, and information-processing devices making use of quantum nanostructures.

(Received May 14, 2007; revised August 31, 2007)